

# SMARTCARB

## Technical note

### Response to questions raised at Midterm Review, 4-5 September 2017, ESTEC

Version 1.0 (2 October 2017)

prepared by Gerrit Kuhlmann and Dominik Brunner

#### Purpose of the document

This document answers the following questions that came up at the SMARTCARB Midterm Review meeting:

- Were XCO<sub>2</sub> columns computed correctly, which for Berlin seem to be low compared to previous studies?
- Is there a consistency between the Berlin emissions in the inventory, the emissions processed as input for the model, and the actual mass of CO<sub>2</sub> in the simulations?
- What is the origin of the small-scale fluctuations in the background CO<sub>2</sub> field?

#### Summary of main findings

- The CO<sub>2</sub> simulated in the model is fully consistent with the emissions in the inventory.
- Emissions of the city of Berlin considered in SMARTCARB are about a factor two smaller than those assumed in previous studies. Emissions in summer are further reduced due to reduced energy demand for heating.
- XCO<sub>2</sub> columns are computed correctly.
- An issue of double-counting of strong point-source emissions in Berlin was detected: Correct emissions and XCO<sub>2</sub> columns should thus be somewhat *lower* than presented at the meeting. In particular, the plumes from the large point sources in Berlin will be less prominent when this error is corrected.
- The variations in background XCO<sub>2</sub> are due both to fluctuations in humidity (not properly accounted for when computing dry air mixing ratios) and vertical overturning in convective cells.

Each of these points will be addressed in detail in the following sections.

## 1. Comparison of emissions and XCO<sub>2</sub> columns over Berlin with LOGOFLUX

The XCO<sub>2</sub> plumes of the city of Berlin simulated in SMARTCARB appear to be weaker than those simulated in the LOGOFLUX project and as published by Pillai et al. (2016). Figure 1 and Figure 2 compare the CO<sub>2</sub> emissions and a selected plume in the two projects, respectively. Since the simulations were conducted for different time periods, a direct comparison is not possible, but the smaller amplitude of the plume in the SMARTCARB simulation is obvious. In the following, we investigate possible reasons for these differences.

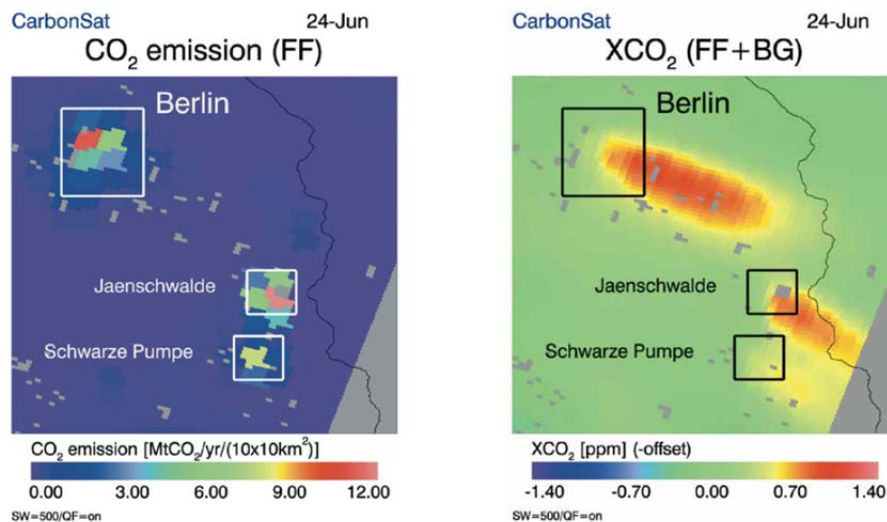


**Figure 1:** CO<sub>2</sub> emissions (left) and XCO<sub>2</sub> plume (right) as simulated in LOGOFLUX (LOGOFLUX, 2015).

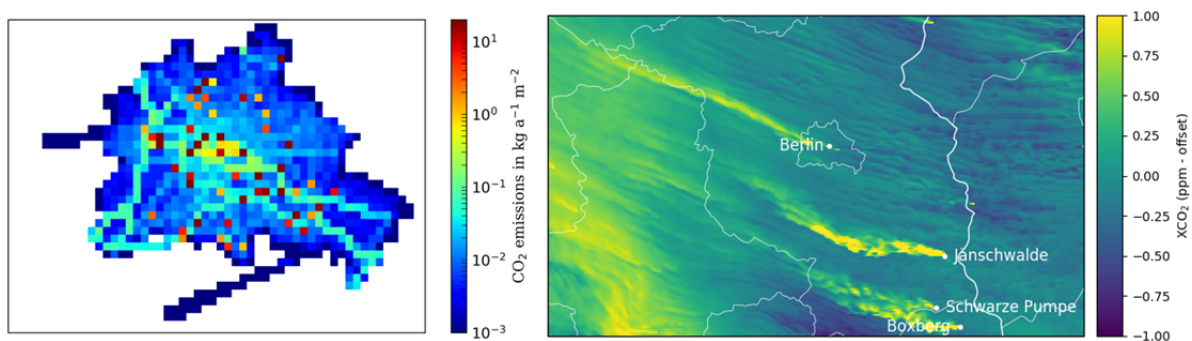


**Figure 2:** CO<sub>2</sub> emissions (left) and XCO<sub>2</sub> plume (right) as simulated in SMARTCARB (2 July 2015, 11 UTC).

In the SMARTCARB simulation presented at the MTR, annual mean emissions from the city of Berlin (Figure 2) were 23.7 Mt CO<sub>2</sub> yr<sup>-1</sup>. Due to the seasonal, weekly and diurnal emission profiles applied in the simulations, the emissions corresponding to the XCO<sub>2</sub> distribution shown in Figure 3 (i.e. 2 Jul 2015 11 UTC) were slightly lower, 21.4 Mt yr<sup>-1</sup>. Emissions in summer are on average 15% lower compared to the annual mean. The SMARTCARB simulations are based on a merged data set combining the TNO/MACC-III inventory outside of Berlin with the inventory of the Senatsverwaltung of the city of Berlin (see SMARTCARB deliverable D1).

Table 1 presents an overview of the CO<sub>2</sub> emissions of Berlin according to the inventory of the Senatsverwaltung of Berlin. Total emissions are 16.8 Mt CO<sub>2</sub> yr<sup>-1</sup>, which is lower than the emissions in the simulation. A closer investigation revealed that some major point sources

(SNAP 1) in the city were represented twice, on one hand as area and on the other hand as single point sources. After eliminating this double-counting, annual mean emissions in the files processed for SMARTCARB are 16.8 Mt CO<sub>2</sub> yr<sup>-1</sup>, consistent with the inventory.

**Table 1:** CO<sub>2</sub> emissions by SNAP category from Berlin emission inventory. Emissions for installations subject to licensing („genehmigungspflichtige Anlagen“) have be re-distributed to appropriate SNAP categories.

SNAP	Name	CO <sub>2</sub> emissions (tons per year)	Remarks
1	Combustion in energy and transformation industries	7'581'324	
2	Non-industrial combustion plants	5'820'281	mainly commercial, institutional and residential heating
3	Combustion in manufacturing industry	228'628	
4	Production processes	169'806	incl. construction sites
5	Extraction and distribution of fossil fuels and geothermal energy	135	
6	Solvent and other product use	0	
7	Road transport	2'721'754	emissions of minor roads were estimated from major roads (see SMARTCARB Deliverable D1)
8	Other mobile sources and machinery	296'069	
9	Waste treatment and disposal	2'763	
10	Agriculture (w/o sinks)	0	
	<b>Sum</b>	<b>16'791'597</b>	

For LOGOFLUX, total annual emissions from Berlin were assumed to be 43 Mt CO<sub>2</sub> yr<sup>-1</sup>, more than twice the value of the city inventory. There are several reasons for this difference: First of all, LOGOFLUX simulations were based on the EDGAR v4.1 inventory for the year 2008. Pillai et al. (2016) already noted that EDGAR had significantly larger emissions over the domain of Berlin than the IER inventory of the University of Stuttgart, despite the fact that the latter was provided for the year 2000 when emissions were higher than in 2008 (see Figure 5). The inventory used in SMARTCARB is representative for the year 2012, when emissions were slightly little lower than in 2008.

**Kohlenstoffdioxid-Emissionen nach Sektoren (Quellenbilanz) 1990 bis 2014**

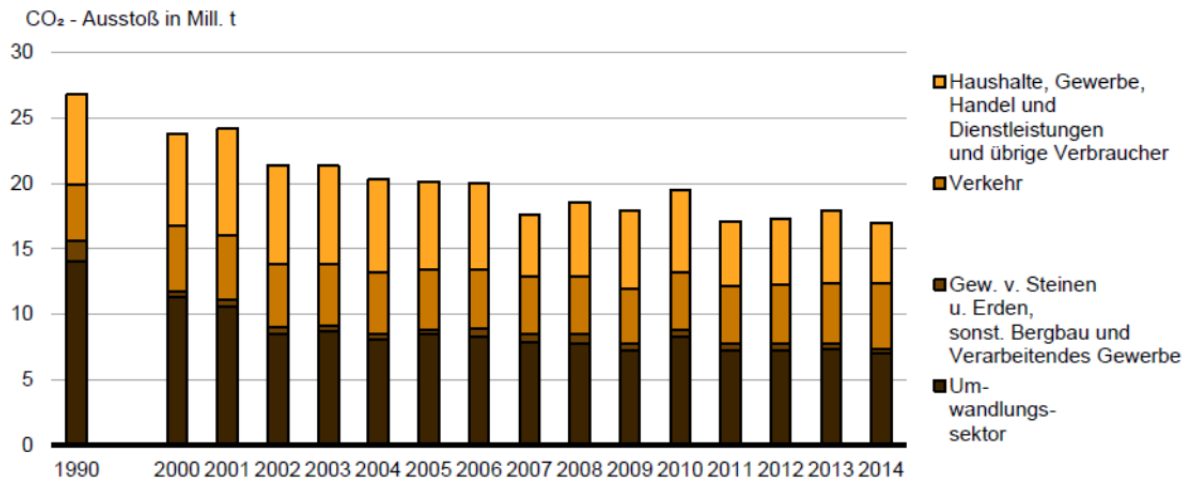


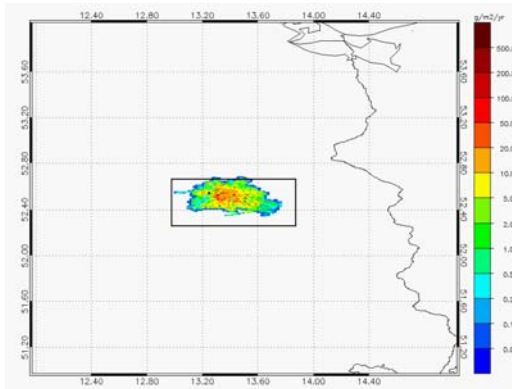
**Figure 3:** Evolution of CO<sub>2</sub> emissions (in Mt CO<sub>2</sub> yr<sup>-1</sup>) in the city of Berlin 1990-2014 (Amt für Statistik Berlin Brandenburg, 2017).

A second reason is that the domain enclosed by the white box in Figure 1 does not only comprise emissions from the city. To further analyze this factor, we compared the emissions within the city boundaries with those in a wider rectangle as shown in Figure 4. Total emissions on 3 Aug 2015, 10 UTC were 14.2 Mt yr<sup>-1</sup> in the city of Berlin (Figure 4a), and 19.6 Mt yr<sup>-1</sup> within the white rectangle (Figure 4b), thus 38% higher. The annual mean value within the white rectangle would be about 15% higher, thus about 23 Mt yr<sup>-1</sup>.

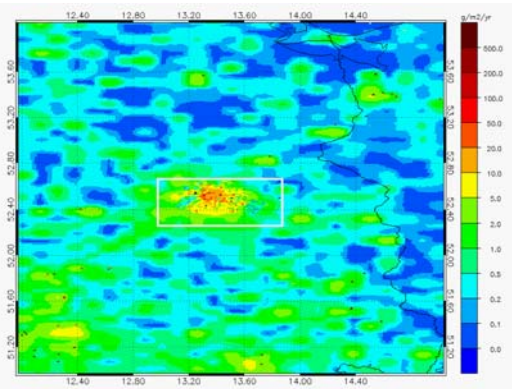
For comparison, annual mean emissions in EDGAR v4.2FT2010 (Figure 4c) over the same domain were 38.8 Mt yr<sup>-1</sup> and in TNO/MACC-III (Figure 4d) were 24.6 Mt yr<sup>-1</sup>. The TNO/MACC-III emissions over Berlin are broadly consistent with the inventory of the city of Berlin, whereas EDGAR is nearly 70% too high. One reason for overestimation could be an erroneous spatial allocation of Germany's CO<sub>2</sub> emissions using population density as a proxy and not accounting for the fact that per capita emissions are lower in large cities. Per capita emissions in Berlin, for example, are about a factor two lower than the German average (Amt für Statistik Berlin Brandenburg, 2017).

A third reason for the lower XCO<sub>2</sub> columns in SMARTCARB is that emissions were treated in 3D, whereas in LOGOFLUX all CO<sub>2</sub> was released at the surface. Because of increasing wind speeds with altitude, the dilution of CO<sub>2</sub> is stronger when CO<sub>2</sub> is released well above the surface, which is a relevant factor for Berlin due to the large contribution of point sources.

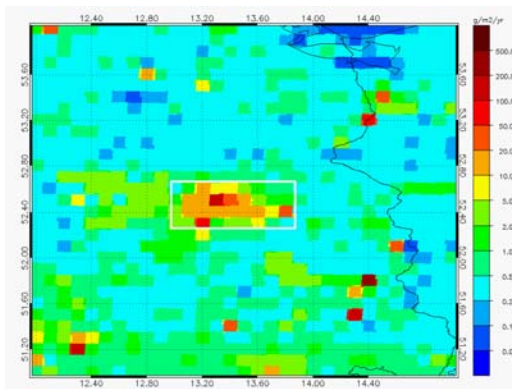
a) Berlin city inventory



b) Berlin inventory merged with TNO/MACC-III



c) EDGAR v4.2FT2010 inventory



d) TNO/MACC-III

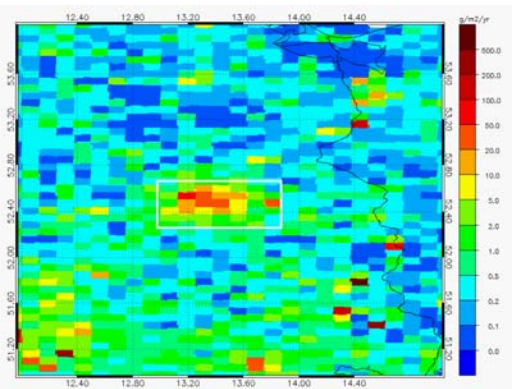


**Figure 4:** Comparison of emissions as used in SMARTCARB for the year 2012 (top row) with EDGAR v4.2FT2010 for 2010 and TNO/MACC-III for 2011 (bottom row). Note that the TNO/MACC-III emissions in figures b) and d) are identical, except that for SMARTCARB individual point sources were assigned to a single 1 km x 1 km grid cell, whereas in panel d) these emissions were smeared out over areas corresponding to the resolution of the TNO/MACC-III inventory. Another difference is the type of interpolation, which is linear in case of b) but nearest-neighbor in case of d). The type of interpolation changes total domain emissions in the domain by less than 0.5%.

To study the effect of distributing emissions vertically, an additional CO<sub>2</sub> tracer is included in the SMARTCARB simulations which is only released at the surface. XCO<sub>2</sub> columns in the Berlin plume are typically 5-20% higher for this tracer, but occasionally more than 50%.

Another major difference is the resolution of the simulations. LOGOFLUX simulations were conducted with the WRF-CHEM model at a spatial resolution of 10 x 10 km<sup>2</sup>, SMARTCARB simulations with the COSMO-GHG model at 1 x 1 km<sup>2</sup> resolution. As a result, the plumes from Berlin and the power plants simulated in LOGOFLUX were broader and resembling Gaussian plumes, whereas the SMARTCARB plumes are sharper and reveal meandering patterns. Furthermore, the plumes generated by the three largest point sources in Berlin become distinct and dominant features, whereas in LOGOFLUX they were mixed with all other sources.

In conclusion, the plumes simulated in LOGOFLUX were more prominent because of approximately 70% higher emissions and because all CO<sub>2</sub> was released at the surface. They were also broader because of 100 times (in terms of area) lower resolution.

## 2. Consistency between inventory and simulations

The processing of emission data involves several steps, each being a potential source of error. Emissions are originally provided as annual fields per species and source category. These fields are then converted to hourly emissions using category-specific time functions, and finally added up to get the total emission of the species in a given hour. These hourly emission fields are further processed and interpolated to the model grid by the COSMO pre-processor tool INT2LM. During a COSMO simulation, this pre-processed emission input is read in at hourly time steps, added to the 3D tendency of moist air mass mixing ratios of the given species, and transported by the model. Finally, the simulated mass mixing ratios are written out once per hour.

To check the consistency along this processing chain, the conservation of mass was checked for the following six steps:

1. Projection of the shapefiles (points, lines and areas) of the Berlin inventory onto the 3D COSMO grid.
2. Projection of the TNO/MACC-III point and area emissions onto 3D COSMO grid.
3. Replacement of TNO/MACC-III emissions over domain of Berlin by emissions from the Berlin inventory.
4. Application of time profiles to the merged emissions.
5. Conversion of hourly emission fields into COSMO-compatible format by INT2LM pre-processor.
6. Ingestion of emissions of a given tracer into COSMO model and subsequent transport of the tracer.

No issue was detected in all these steps, except for a double-counting of some point sources in Berlin as mentioned earlier. This error affects the simulations for January and July 2015 (CO<sub>2</sub> in the Berlin plume is too high) but has been corrected for all other months. The total domain emissions of the Berlin tracer obtained after steps 1-5 is still the same as initially.

To check the consistency between emissions and the tracer in the COSMO model (step 6), the total tracer mass in the model domain was compared with the cumulated emissions. Figure 5 shows the cumulated emissions and the total mass in the model domain for the tracers representing the large power plants and the city of Berlin. They agree well in the first few hours of the simulation when the tracer mass is building up within the model domain, but they start to diverge after a few hours when the tracers start leaving the model domain. In summary, the mass of CO<sub>2</sub> simulated in the model is fully consistent with the original emissions.

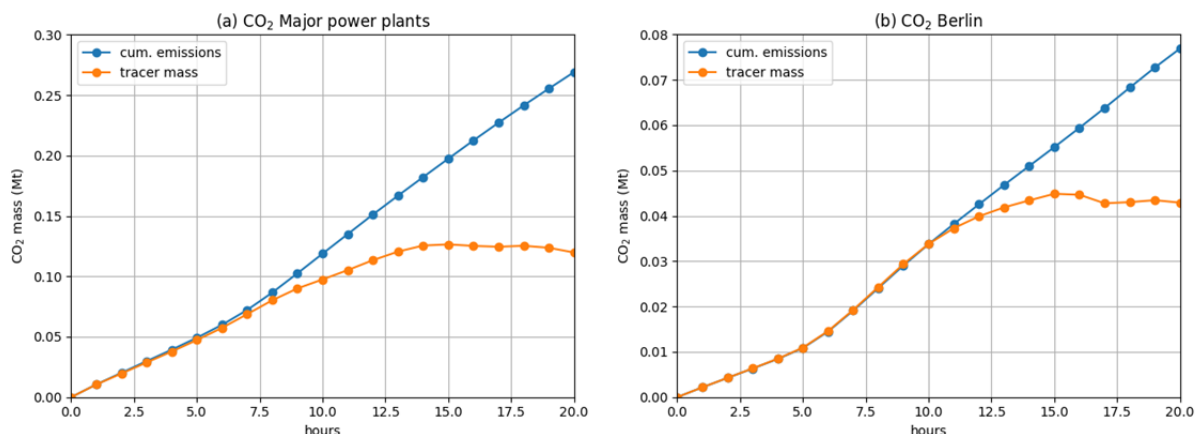


**Figure 5:** CO<sub>2</sub> mass of (a) large power plants and (b) Berlin from cumulated emission files and in COSMO output files.

We also checked whether the column mean dry air mixing ratios XCO<sub>2</sub> are correctly calculated. For this we compared the results of two completely independent derivations (Python code by G. Kuhlmann, IDL code by D. Brunner), which showed negligible differences ( $\sigma < 0.002$  ppm). The largest uncertainty is the extrapolation to the top of the atmosphere, since the model domain only extends to about 25 km. However, this uncertainty is very small. Furthermore, any major error would be readily visible in the background CO<sub>2</sub> tracer (tracer constrained at domain boundaries by global CAMS fields). The values of this tracer are close to 400 ppm as expected.

### 3. Small-scale fluctuations

The background XCO<sub>2</sub> fields, although constrained by coarse-resolution global model fields, show unexpected small-scale fluctuations in the form of stripes, most clearly around noon in summer (see Figure 6). These fluctuations also appear in other model variables, notably in specific humidity, (vertical) wind speeds (Figure 8) and heights of the planet boundary layer (Figure 9).

COSMO tracer fields are transported as specific masses (kg CO<sub>2</sub> per kg moist air). The CAMS CO<sub>2</sub> fields, however, were provided as dry air mole fractions. Instead of converting these boundary condition values to moist mixing ratios at the beginning and back to dry mixing ratios when writing out the fields, we decided not to apply any of these conversions, assuming that the influence is small for column XCO<sub>2</sub>. However, since the fluctuations also appear in specific humidity, it is possible that the fluctuations are caused by fluctuations in the dry to moist air mass ratios.

In the following, we briefly describe how XCO<sub>2</sub> is computed from the COSMO fields:

Assuming hydrostatic equilibrium, the weight of moist air in the volume per m<sup>2</sup> (i.e. the partial column of moist air), is obtained from the pressure difference at the bottom and top of the volume as

$$M_k^{\text{air}} = \frac{p_{k+\frac{1}{2}} - p_{k-\frac{1}{2}}}{g}$$

with  $g$  the constant of gravity and  $p$  the pressure (Pa) at half levels of the model. The partial column of dry air is obtained by subtracting the mass of water vapor, i.e.

$$M_k^{\text{dry}} = M_k^{\text{air}} - M_k^{\text{air}} Q_k = M_k^{\text{air}} [1 - Q_k]$$

with specific humidity  $Q_k$ . The partial column of CO<sub>2</sub> is obtained as

$$M_k^{\text{CO}_2} = M_k^{\text{air}} \cdot s\text{CO}_{2k}$$

where  $s\text{CO}_{2k}$  is the specific mass of CO<sub>2</sub> (kg CO<sub>2</sub> / kg moist air) at model level  $k$ .

Finally, the column mean dry air mole fraction is obtained by summing up the masses of dry air and of CO<sub>2</sub> over all levels  $k = 1 \dots K$ :

$$\text{XCO}_2 = \frac{\sum_k M_{\text{CO}_2}(k)}{\sum_k M_{\text{dry}}} \cdot \frac{m_{\text{dry}}}{m_{\text{CO}_2}} = \frac{\sum_k \left[ p_{k+\frac{1}{2}} - p_{k-\frac{1}{2}} \right] s\text{CO}_{2k}}{\sum_k \left[ p_{k+\frac{1}{2}} - p_{k-\frac{1}{2}} \right] [1 - Q_k]} \cdot \frac{m_{\text{dry}}}{m_{\text{CO}_2}}$$

with molar weights of dry air ( $m_{\text{dry}} = 28.97$  g/mol) and CO<sub>2</sub> ( $m_{\text{CO}_2} = 44.01$  g/mol).

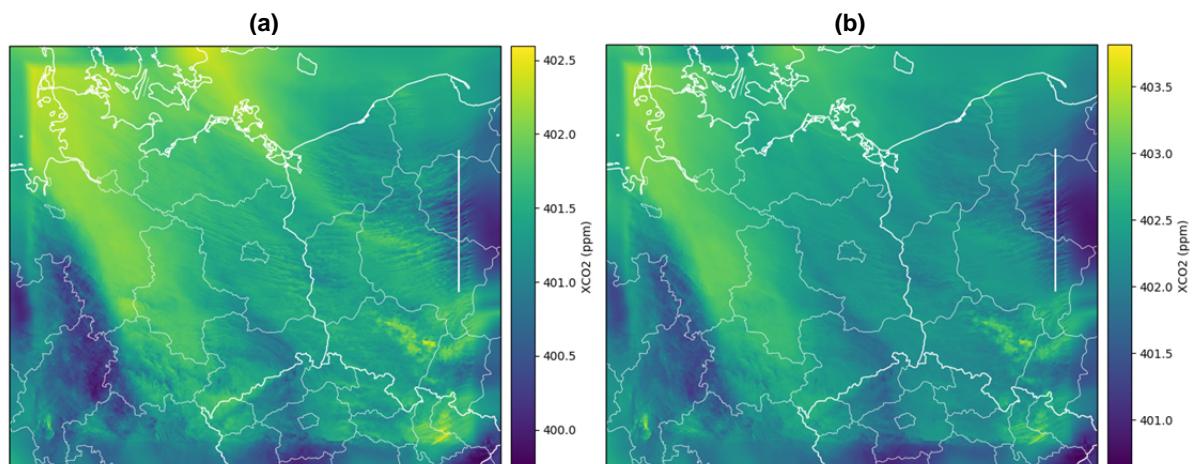


**Figure 6:** The XCO<sub>2</sub> background field (XCO2\_BG tracer) for (a) moist air and (b) dry air (2.7.2015, 11 UTC).

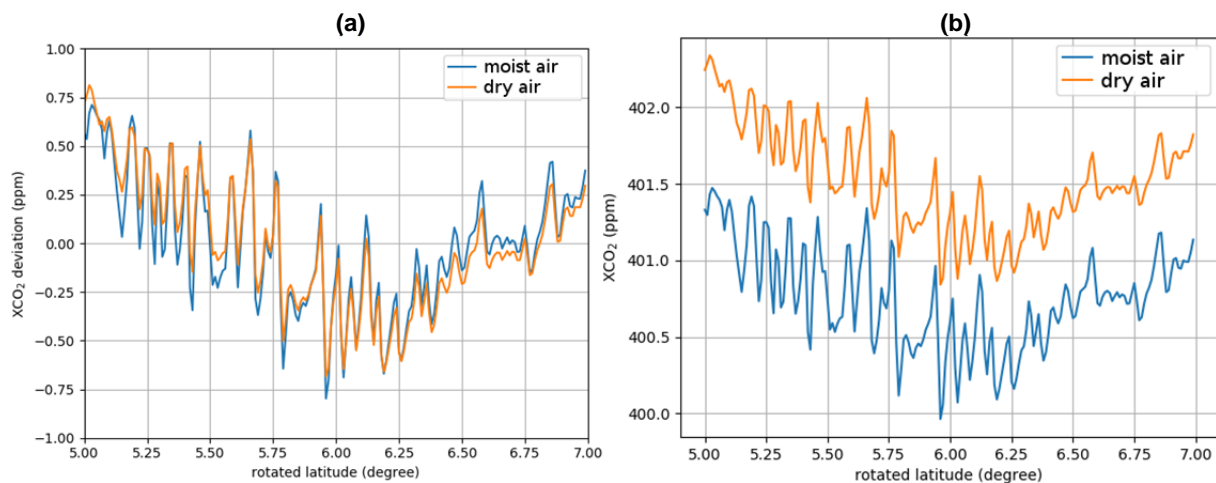


**Figure 7:** Cross section in XCO<sub>2</sub> background (see Figure 6) for moist and dry air. (a) Deviation from the mean. (b) Absolute values.

Since specific humidity shows similar stripes as the XCO<sub>2</sub> fields, ignoring the contribution of humidity to the layer masses ( $Q_k = 0$ ), as done for the figures presented at the MTR, might cause these stripes. Therefore, we recalculated the XCO<sub>2</sub> fields accounting for the effect of humidity. Figure 6 shows the XCO<sub>2</sub> field with and without accounting for humidity. The difference between the maps is small, as seen more clearly in a north-south cross section (Figure 7). Overall, accounting for the effects of humidity results in a slightly smoother field, but most of the fluctuations remain and thus must have a different origin. The most likely reason is vertical redistribution of CO<sub>2</sub> in convective cells, which can only affect the columns if the background CO<sub>2</sub> has a vertical gradient. We therefore made an additional test with constant initial and boundary conditions of CO<sub>2</sub>. Figure 10 shows the corresponding XCO<sub>2</sub> field with and without including humidity in the calculations.



**Figure 8:** Mean vertical wind speed (2 July 2015, 11 UTC).

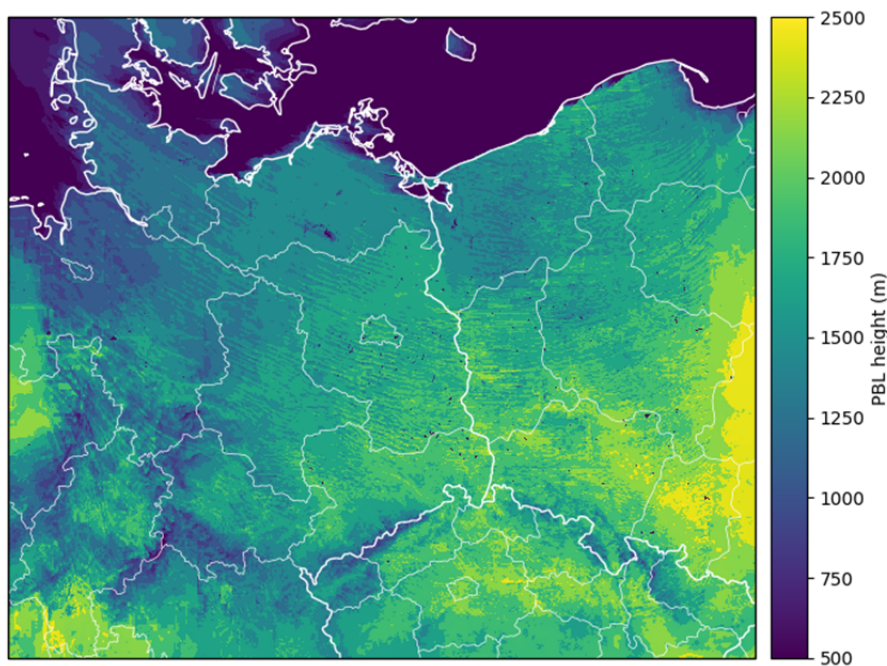


**Figure 9:** Height of planetary boundary layer (PBL) (2 July 2015, 11 UTC).

Figure 10 indicates that when CO<sub>2</sub> is initialized as a constant 3D field and transported as moist mass mixing ratios, the distribution in the model remains flat, i.e. the moist mass mixing ratios are (almost) perfectly conserved. When treated as dry air mass mixing ratios, however, stripes appear due to small-scale fluctuations in the vertical column of humidity. The amplitude of these stripes, however, is significantly smaller than in Figure 6, suggesting that the main reason for the stripes is indeed vertical redistribution of CO<sub>2</sub> in convective rolls, as nicely illustrated at <http://www.ryanhanrahan.com/tag/horizontal-convective-rolls/>.

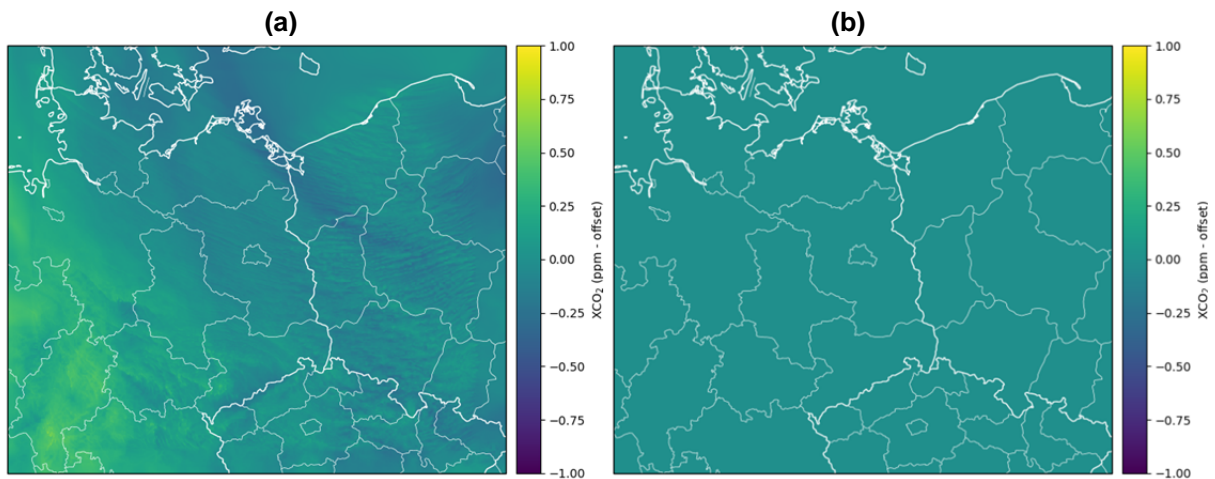


**Figure 10:** XCO<sub>2</sub> background field (a) without and (b) with including humidity for constant initial and boundary conditions ( $6 \times 10^{-6}$  kg CO<sub>2</sub> / kg moist air).

#### References:

LOGOFLUX-2, Final report of CarbonSat Earth Explorer 8 Candidate Mission “LOGOFLUX 2 - Flux Inversion Performance Study“, NOVELTIS, Version 1.1, 12 October 2015.

Pillai, D., Buchwitz, M., Gerbig, C., Koch, T., Reuter, M., Bovensmann, H., Marshall, J., and Burrows, J. P.: Tracking city CO<sub>2</sub> emissions from space using a high-resolution inverse modelling approach: a case study for Berlin, Germany, *Atmos. Chem. Phys.*, 16, 9591-9610, <https://doi.org/10.5194/acp-16-9591-2016>, 2016.

Statistischer Bericht, E IV 4 – j / 14, Energie- und CO<sub>2</sub>-Bilanz in Berlin 2014, Amt für Statistik Berlin-Brandenburg, Potsdam, 2017.

URL: [https://www.statistik-berlin-brandenburg.de/publikationen/stat\\_berichte/2017/SB\\_E04-04-00\\_2014j01\\_BE.pdf](https://www.statistik-berlin-brandenburg.de/publikationen/stat_berichte/2017/SB_E04-04-00_2014j01_BE.pdf), last accessed 30/09/2017.